The Pierre Auger Observatory: results and open issues

D. Martello[a], for the Pierre Auger Collaboration[b]

[a] *Dep. of Mathematics and Physics "E. De Giorgi" and INFN Lecce*
[b] *Observatorio Pierre Auger, Av. San Martín Norte 304, 5613 Malargüe, Argentina*
(Full author list : http://www.auger.org/archive/authors_2013_05.html)

Abstract

We will present the status and the main results of the Pierre Auger Observatory. These include the measurement of the cosmic ray energy spectrum above 10^{18} eV, where we observe a suppression for energies larger than 5.5×10^{19} eV, the analyses of the arrival directions and the chemical composition. The implications on the origin and on the acceleration mechanisms of the most energetic cosmic rays will be discussed with a particular emphasis to the still open issues.

Keywords:
high energy cosmic rays, energy spectrum, primary composition, sources

1. Introduction

Cosmic rays are ionized atomic nuclei reaching the Earth from outside the Solar System. Although discovered in 1912, their sources and propagation mechanisms are still the subject of intense research.

Understanding the sources, nature and propagation properties of the cosmic rays at ultra high energies ($E > 10^{18}$ eV) is one of the key questions in astroparticle physics. From the experimental point of view, their study can be performed indirectly, by exploiting the extensive air showers (EAS) they produce by interacting with the nuclei in the Earth's atmosphere. Among the different features characterizing the spectral shape, the region between $\simeq 10^{18} - 10^{19}$ eV is thought to provide information on the ultra high energy cosmic rays (UHECR).

Anyway, the all particle spectrum cannot provide a discrimination among the different astrophysical hypotheses, and the determination of the primary composition is mandatory to reach any reliable conclusion. Analysis of the arrival directions and their anisotropy can give further insight into the sources and provide information about the magnetic fields which the ultra high energy cosmic rays experience during their travel to Earth.

2. The Pierre Auger Observatory

The Pierre Auger Observatory, located near Malargüe in the province of Mendoza in Argentina (Fig. 1), consists of an array of 1660 water-Cherenkov surface detectors (SD) [1] deployed on the ground over a triangular grid of 1.5 km spacing and covering an area of $\simeq 3000$ km^2. Each SD station is a polyethylene tank of cylindrical shape with size 10 m$^2 \times 1.2$ m, filled with purified water. Cherenkov light produced by charged particles of EAS in the water is detected by three 9" photomultipliers. Each station is autonomous with a battery and a solar panel. The signals are digitized locally and the information is transmitted via radio to the central data acquisition system. Synchronization is provided by the standard GPS system. The surface detector measures the front of a shower as it reaches the ground. The stations activated by the event record the particle density and the time of arrival.

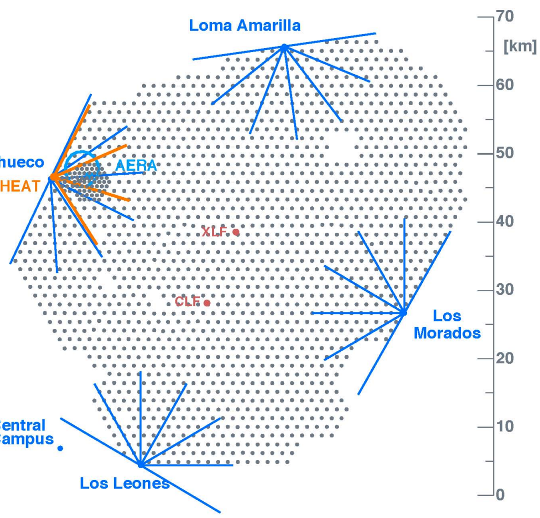

Figure 1: The Pierre Auger Observatory located near Malargüe, Province of Mendoza, Argentina. The FoVs of the fluorescence telescopes (blue/orange radial lines) cover the water Cherenkov surface detector array (dots).

The ground array is overlooked by 27 fluorescence telescopes, grouped in four sites, making up the fluorescence detector (FD). In each fluorescence telescope the light is collected by a segmented spherical mirror of area 3.6 m×3.6 m through a UV-transparent filter window and a ring corrector lens. Each camera consists of 440 hexagonal photomultipliers, each with a field of view of 1.5°.

The surface array and the fluorescence detector provide complementary measurements of the extensive air showers. The SD samples the density of secondary shower particles at the ground. For each event, the particle density is expressed in units of a vertical-equivalent muon, the average signal produced by vertically incident muons. Measurement of the arrival time of the particles of the shower front at the SD allows one to determine the cosmic ray arrival direction while the estimated total size of the shower is proportional to the energy of the primary cosmic ray.

The FD measures the longitudinal development of the EAS in the atmosphere by detecting the fluorescence light emitted by de-excitation of atmospheric nitrogen molecules excited by the charged particles of the shower. The result is a measurement of the energy deposit as a function of the atmospheric depth, as in a calorimeter. As opposed to the SD array, the FD may only operate during clear, moonless nights and its duty cycle is thus reduced to about 14%. Since the fluorescence emission, as well as the light scattering and attenuation, depends on atmospheric conditions, several systems monitor the weather conditions, the aerosol content and the cloud coverage [2].

Events detected by at least one FD telescope and one SD station are named *hybrids*. The combination of the timing information from the FD and the SD provides an accurate determination of the geometry of the air showers. In fact, in hybrid mode the arrival direction of the primary particle and the impact point of the shower at the ground are determined with a resolution of about 0.6° and 50 m, respectively. A sub-sample of events recorded and independently reconstructed by both FD and SD detectors can be used to calibrate the energy scale of the SD array [3]. This provides an energy parameter only weakly dependent on the primary composition and on the hadronic interaction models.

3. Energy Spectrum

The energy spectrum above 2.5×10^{18} eV has been determined using mainly the data from the SD [4], considering only events up to 60°. The SD events were collected between 1 January 2004 and 30 December 2010, with a total exposure of 20905 km^2 sr yr. The exposure is obtained by integrating the number of active stations over time; the overall acceptance uncertainty is $\simeq$ 3% [5]. Despite the low duty cycle of the FD, the energy spectrum has been extended to 10^{18} eV using hybrid events, thanks to the good energy resolution and low threshold, thus investigating the transition from galactic to extragalactic in detail [6]. The hybrid events were taken between 1 November 2005 and 30 September 2010. The total systematic uncertainty in the energy scale is about 22%, the main contribution coming from the uncertainty in the fluorescence yield (14%) and in the reconstruction of the longitudinal profile (10%).

The SD and hybrid spectra can be combined using a maximum likelihood method, since both have the same systematic uncertainties in their energy scale. The normalization uncertainties are, on the contrary, independent and have been used as additional constraints in the procedure. The resulting spectrum is shown in Fig.2; a fit with three power laws is shown by the dashed lines, while the solid line indicates the result of a fit with two power laws and a smooth function. It is possible to see that there are two clear spectral features: the ankle at $\log_{10}(E_{ankle}/\mathrm{eV}) = 18.62 \pm 0.01$ and a strong suppression above $\log_{10}(E/\mathrm{eV}) = 19.63 \pm 0.02$. The suppression is seen with a significance of 20 σ. Different astrophysical models can explain these features. The ankle could be due to e^+e^- pair production of protons with the photons of the cosmic microwave background (CMB) [7], or more traditionally to the intersection of a steep galactic component and the onset of a flatter extra-galactic one [8]. At even higher energies, the cutoff could be due to photo-pion production of extragalactic protons in the CMB (the GZK cutoff [9]), although the same feature could arise when reaching the limits in the maximum energy of the sources.

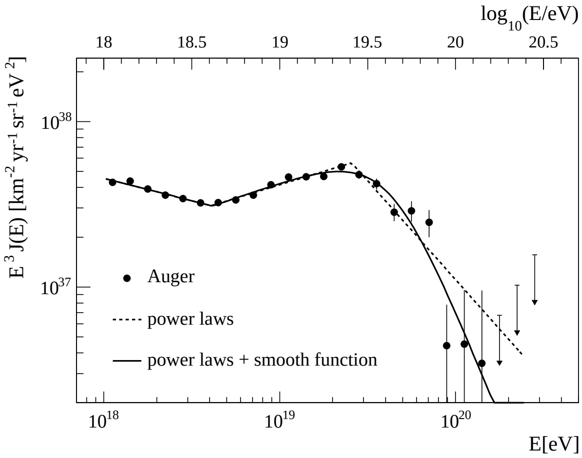

Figure 2: The combined Auger energy spectrum. Only statistical uncertainties are shown. The systematic uncertainty on the energy scale is 22%.

A comparison of the Auger results with data from HiRes, Telescope Array and Yakutsk has been recently performed [10]. The various fluxes can be rescaled assuming that any difference among them is due solely to their energy scale and not to aperture calculations or energy resolution. The differences found are entirely consistent with the systematic energy uncertainties quoted by the experiments.

The Auger energy spectrum in figure 2 can be described by both a heavy or proton composition at the highest energies and the spectral information must be complemented by independent measurements of the primary composition.

4. Mass Composition

The UHECR mass composition is another key aspect to understand their origin and propagation. It can be inferred through observables related to the EAS development. In Pierre Auger data, one of the most sensitive variables is the depth of the shower maximum, X_{max}. Proton induced showers will have, on average, deeper X_{max} with larger fluctuations, with respect to iron primaries. The X_{max} can be measured directly by the FD looking at the longitudinal energy deposit profile on an event-by-event basis. The statistics is however limited at the highest energies. X_{max} can also be inferred from related variables at the ground using the SD.

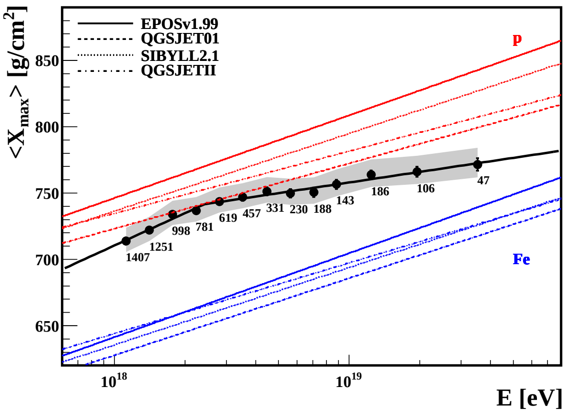

Figure 3: < X_{max} > as a function of energy, compared with the predictions of air shower simulations using different hadronic interaction models.

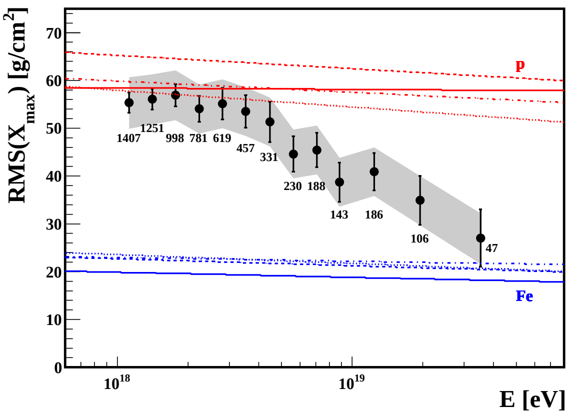

Figure 4: RMS(X_{max}) as a function of energy, compared with the predictions of air shower simulations using different hadronic interaction models.

The average of the X_{max} distribution as a function of energy measured by the FD, < X_{max} >, and the RMS(X_{max}) [11], are shown in figure 3 and 4. The depth of shower maximum depends on the hadronic interactions that rule the shower development. Therefore, the predictions of different hadronic interaction models for these observables are shown, both for proton and iron induced showers. One can observe that there is a trend towards a heavier composition at the highest energies, even though the analysis of < X_{max} > and RMS(X_{max}) suggests a complex mass composition scenario [12].

SD observables, such as the asymmetry of the SD signal risetime [13] are sensitive to primary mass composition, but on a statistical basis. Additionally, the reconstruction of the muon production depth profile can be done using the SD, on an event-by-event basis for inclined events, with zenith angle around 60° [14]. This is done using the shower geometry and muon arrival times to the ground, with respect to the shower front. The depth of the maximum of this profile, X_{max}, provides another observable sensitive to the mass composition. At present, these SD observables support at the highest energies the trend measured with the FD. The new hadronic interaction models, which have been re-tuned to describe the LHC data (EPOS-LHC and QGSJET-II-04), are now more similar to each other, but the general trends with respect to data remain unchanged.

Some consequences from the astrophysical point of view can be derived from our data. Extragalactic sources of protons seem to be disfavored by our composition result, within the uncertainties on the hadronic interaction models used to interpret the data. In a propagation scenario, nuclei from nearby sources could produce small mass dispersion at Earth, as propagation would not be able to degrade mass and energy. If on the other hand the proton component is depleted by the reach of a rigidity dependent end of the injection spectrum, and if sources are uniformly distributed, hard injection spectra with low energy cutoffs, together with local sources, could explain the data [15, 16].

A different conclusion, leading to a light composition up to the highest energies, has been drawn from the data of HiRes and the Telescope Array. However, a direct comparison of their results with the Auger ones is not yet possible, as the detector biases are included in their simulation. Furthermore, their datasets are substantially smaller than that of Auger. A lengthy discussion about this comparison can be found in [17].

5. Number of Muons at Ground

The muon content of the shower is not only sensitive to the mass composition of the primary but is also an important tool to probe the hadronic interactions that occur during the shower development, as muons are the direct decay product of mesons (mainly pions and kaons). Once muons are produced, they have a large probability of reaching the ground without interacting. In the Pierre Auger Observatory there are several strategies to measure the number of muons at the ground. Firstly one can distinguish direct and indirect measurements. The direct measurements rely on the analysis of time traces of the SD stations. For inclined showers ($\theta > 60°$), the signal measured by an SD station is dominated by muons, as most of the electromagnetic component is attenuated during the shower development in the atmosphere. Hence, the number of muons can be extracted by fitting the shower footprint at the ground with simulations [18]. For more vertical events ($\theta < 60°$), the measurement can be done either by identifying muons or, by subtracting the electromagnetic component from the total signal of the FADC traces. Muon counting is achieved using a multivariate analysis that was trained with simulations to identify the muon peaks in the SD traces. The second approach is the so-called smoothing method which is based on the fact that the electromagnetic component has a continuous (smooth) signal in time that can be identified and subtracted using a filter algorithm. Indirect methods take advantage of the hybrid technique, i.e., combine FD and SD information. The indirect measurement uses the universality method, which is based on the fact that the muonic signal parameterized as a function of X_{max} and S(1000) is, according to EAS Monte Carlo simulations, independent of the primary mass composition and depends only weakly on the hadronic interaction model.

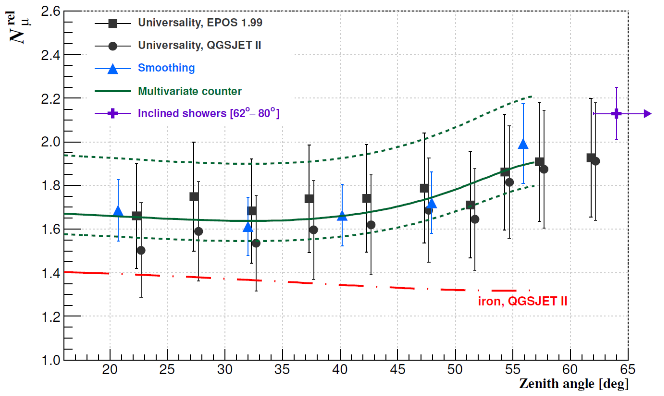

Figure 5: Number of muons estimated at 1000 m from the shower core relative to the predictions of simulations using QGSJet-II.03 with proton primaries at $E = 10^{19}$ eV. The results are displayed as a function of the zenith angle.

The number of muons, estimated at 1000 m from the shower core, relative to the predictions of simulations using QGSJet-II.03 [19] with proton primaries, N_{μ}^{rel} , is shown in figure 5 for the different analysis methods listed above [20]. All the methods present compatible results, within uncertainties. The number of muons predicted by the models shows a deficit with respect to data, and the deficit increases with zenith angle. This deficit is present even when choosing iron primaries and the hadronic interaction model characterized by having more muons (EPOS1.99 [21]). The main factors that affect this discrepancy between data and Monte Carlo simulations are the uncertainty on the energy scale (currently around 22%), the unknown mass composition and uncertainties on the hadronic models (for instance, potential problems on the muon attenuation). However, none of these provides an easy solution by itself.

6. Searches for Photons

UHE primary photons can provide invaluable information about the astrophysics of cosmic rays. Their detection would be a direct proof of the GZK cutoff; limits on exotic models [22] and tests for new physics [23] could be obtained from a positive or negative result on their detection. Their search is based on the characteristic features of the showers they produce in comparison to the hadronic ones.

Primary photons produce late developing showers, a characteristic further enhanced by the LPM effect [24]. At a given energy, photon initiated showers are expected to develop slower than proton induced showers, due to smaller secondary multiplicities and to the suppression of the cross-section due to the LPM effect. Therefore, one can search for photon events by looking for events with an unexpectedly large X_{max} measured by the FD [25]. The deeper X_{max} is associated to a more dispersed distribution of the arrival time of the particles at ground level. At a given distance from the shower axis, the arrival time of the first particles is delayed with respect to a planar shower front and the radius of curvature is thus expected to decrease for photon induced showers [25]. These observables can be recorded by means of the SD. The upper limits derived from both the SD and the hybrid data collected by Auger are shown in Fig.6 and discussed in [26, 27].

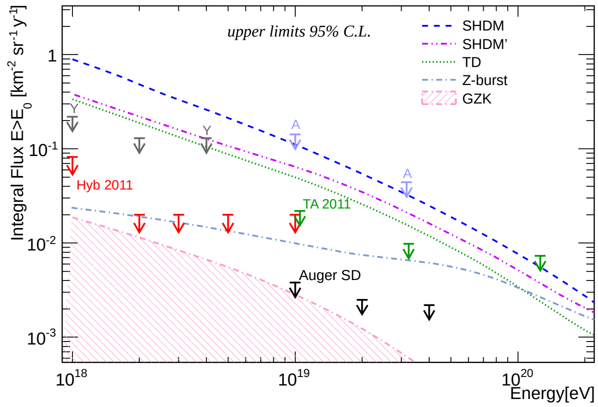

Figure 6: Upper limits on the photon flux derived using hybrid analysis (red arrows) and SD data (black arrows). The shaded region corresponds to the photon flux estimated with the GZK effect assuming a pure proton composition. The lines are the predictions for exotic models.

7. Anisotropies

The angular distribution of the arrival directions of UHE cosmic rays as a function of energy is a key observable to provide information about their sources and nature, complementary to those of energy spectrum and composition. UHE particles are most probably extragalactic, and if the observed cutoff in the spectrum can be attributed to the GZK propagation effect we could expect their sources to be confined in our courtyard, within about 100 Mpc. In 2007 [28] the Auger Collaboration reported the observation of a correlation between the arrival directions of the highest energy cosmic rays and the positions of nearby AGN from the Véron-Cetty-Véron catalog [29]. The result came from an analysis of independent data with a priori parameters determined from an exploratory scan; this avoided the use of penalty factors which would be needed in a posteriori analyses.

The most recent update of this search is shown in Fig.7 [30]: the fraction of correlating cosmic rays is (33 ± 5)% (28 events correlating out of a total of 84). The probability of this correlation occurring by chance if the true distribution of arrival directions is isotropic stays below 1%. The independent averages of 10 consecutive events are also shown by the black dots. A recent comparison of our result with the Telescope Array and Yakutsk data showed that the correlating fractions are compatible [31]. More data are necessary to show whether this correlation is statistically significant or not. Another possible scenario is that the anisotropy is dominated by cosmic rays originating

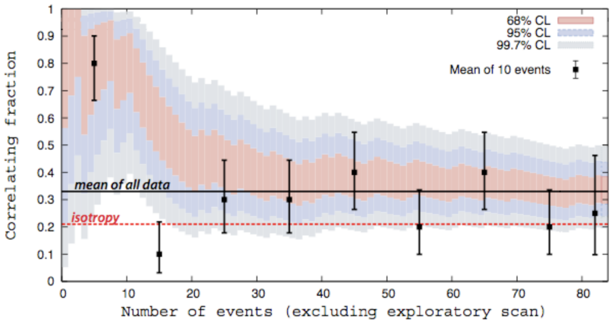

Figure 7: The correlating fraction as a function of the total number of time-ordered events. Different confidence levels are shown, together with the isotropy value $p = 0.21$.

from the vicinity of Centaurus A, the nearest active galaxy, with an estimated distance of about 3.8 Mpc, since 19 events out of 7.6 expected have arrival directions within 24° of CenA. A Kolmogorov-Smirnov test shows that the chance probability for this to happen is 4%. Directionally aligned events, or multiplets, can be expected from the same source after deflection in intervening magnetic fields, showing a correlation between the arrival direction and the inverse of energy. The largest multiplet found was one 12-plet, but, in this case, the probability for it to come from an isotropic distribution is $\simeq$ 6% [32]. Potential sources of galactic cosmic rays have been looked for by performing a blind search for neutron primaries [33]. In fact, due to the relativistic time dilation the UHE neutron mean decay length is (9.2×E/EeV) kpc; above 2 EeV, neutron emitters can be searched for in the whole Galaxy. Auger can detect neutron showers by a simple search for an excess of proton-like showers from a specific direction in the sky.

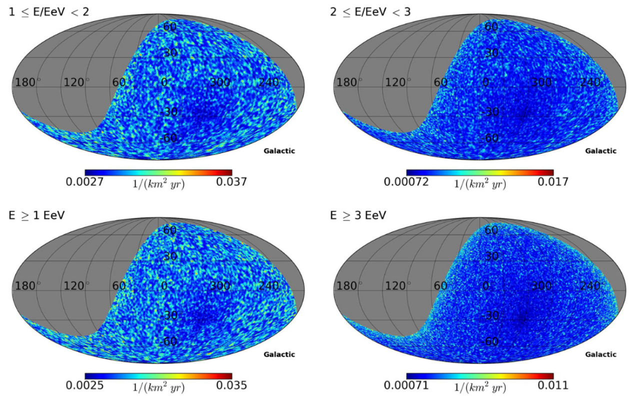

Figure 8: Celestial maps of the neutron flux upper limit (particles/km^{2}yr) in Galactic coordinates.

No candidates have been found, bringing to a median flux upper limit of 0.0114 n km^2 yr^1 above 1 EeV (Fig. 8). The absence of a neutron flux from the Galaxy, which could be expected in the hypothesis of sources steadily emitting protons and neutrons with similar luminosity, could be a hint that the sources at EeV energy could be e.g. extragalactic, transient or of low intensity but numerous and uniformly distributed in the galaxy.

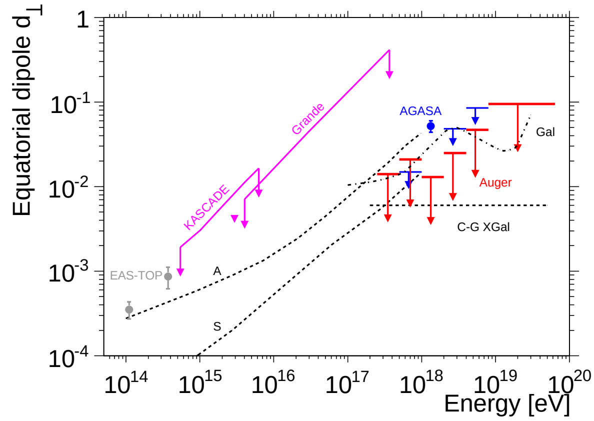

Figure 9: Equatorial dipole component as a function of energy. In red the Auger upper limits.

The large scale distribution of the arrival directions of cosmic rays is another fundamental tool in the search for their origin. The results from a study performed using data from the SD array are shown in Fig.9 [34].

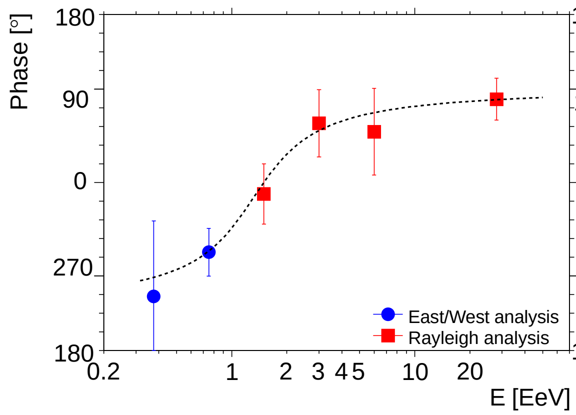

Figure 10: Phase of the first harmonic as a function of energy

No significant anisotropies are observed, resulting in the most stringent bounds on the first harmonic amplitude above $2.5 \cdot 10^{17}$ eV. The limits obtained already exclude some galactic sources models (according to which the cosmic rays at these energies are galactic and can escape by diffusion and drift motion). In extragalactic models the transition is put at the second knee (E$\simeq$ 400 PeV) and their large scale distribution is influenced by the relative motion of the observer with respect to the frame of the source; more data are needed to test these predictions. Interestingly, the phase of the first harmonic shows a smooth transition between a common phase of $\simeq$ 270° below 1 EeV and $\simeq$ 100° above 5 EeV. A consistency of the phase in ordered energy intervals can indeed be expected in presence of a real underlying anisotropy, standing out of the background more prominently than the amplitude (see figure 10 [34]). However, no confidence level can for the moment be assigned to this result, being an a posteriori observation. The study of the large scale anisotropy has been performed for the first time with Auger data as a function of both the right ascension and the declination and expressed in terms of dipole and quadrupole amplitudes [35].

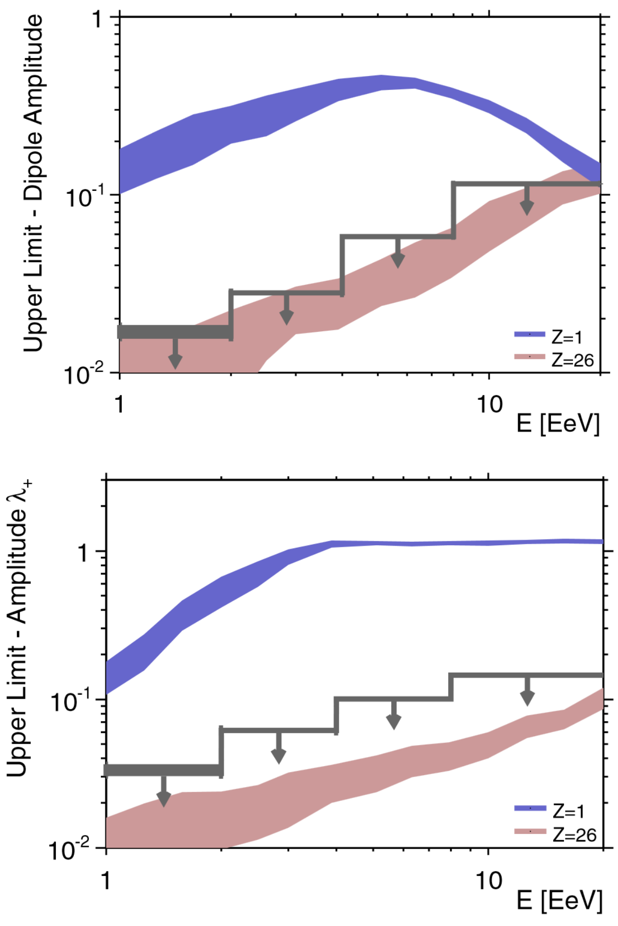

Figure 11: 99% CL upper limits on the dipole and quadrupole momenta as a function of energy. The expectations from a toy galactic disk models are also shown.

No significant deviations from isotropy are detected. Under the hypothesis that any anisotropy is dominated by these moments, 99% CL upper limits can be derived, as shown in Fig.11. As an example of the power of the measurement to discriminate among different astrophysical models, the experimental limits are compared in the figure with the expectations from a toy model, in which the sources of protons and iron are stationary and uniformly distributed in the galactic disk. Since the expected amplitudes for protons are found largely above the allowed upper limits, we can exclude this scenario for the light component of EeV primary cosmic rays.

8. Conclusions and future developments

The Pierre Auger Observatory has reached a cumulative exposure of more than 26000 km^2 sr yr (SD and FD).

The data taken with the Observatory have led to a number of major breakthroughs in the field of ultra-high energy cosmic rays. Firstly, the *ankle* and a suppression of the cosmic ray flux have been established unambiguously. Secondly, due to the Auger limits on the photon flux at ultra-high energy, it is now clear that unusual "top-down" source scenarios, such as the decay of super-heavy particles, cannot account for a significant part to the observed flux. Finally, there are indications of an anisotropic distribution of the arrival directions of particles with energies greater than 5.5×10^{19} eV. These results are consistent with a scenario in which particle acceleration takes place at sites distributed similarly to the matter in the nearby universe. In this scenario, the arrival direction anisotropy as well as the flux suppression is ascribed to the particle energy losses en route to Earth (GZK effect).

However, data on shower development fluctuations as well as other composition-sensitive observables require a rather different interpretation of the Auger data. The observed flux suppression is indicating the upper-limit of the power of the accelerator. It may be that the uppermost end of the cosmic ray energy spectrum is dominated by high-Z particles from a single source or single source population, possibly within the GZK horizon, for which the upper limit of particle acceleration almost coincides with the energy of the GZK suppression.

Moreover, the discrepancy between the expected and measured number of muons currently found calls into question the prediction of the hadronic interaction models and may affect some of the previous conclusions.

All these information about the characteristics of the primary cosmic rays have opened more questions:

- Understand the origin of the flux suppression at the highest energies, i.e., to differentiate between energy losses during extragalactic propagation and the maximum energy of particles injected by sources, either galactic or extragalactic.
- Perform composition driven anisotropy searches. Identify a flux contribution of protons up to the highest energies will be a decisive ingredient for estimating the physics potential of existing and future cosmic ray, neutrino and gamma detectors.
- Determine the energy at which the transition from galactic to extragalactic sources of cosmic rays takes place.
- Identify the origin of the discrepancy currently found between the observed and expected muon numbers. This will play a crucial role in the understanding of the UHE hadronic interactions.

[1] The Pierre Auger Collaboration, Nucl. Instr. Meth. A **620** (2012) 227.
[2] The Pierre Auger Collaboration, Astrop. Phys. **33** (2010) 108.
[3] R. Pesce for the Pierre Auger Collaboration, Proc. 32nd ICRC, Beijing, China (2011) and arXiv: 1107.4809.
[4] The Pierre Auger Collaboration, Phys. Rev. Lett. 101 (2008) 061101.

[5] The Pierre Auger Collaboration, Nucl. Instr. Methods A **613** (2010) 29.
[6] M. Settimo for the Pierre Auger Collaboration, Eur. Phys. J. Plus **127** (2012) 87.
[7] V. Berezinski, A. Gazizov, S. Grigorieva, Phys. Rev. D **74** (2006) 043005.
[8] A. M. Hillas, in Cosmology, Galaxy Formation and Astroparticle Physics on the pathway to the SKA, H.-R. Klöckner, M. Jarvis, S. Rawlings, A. Taylor (eds.) (2006) Oxford, United Kingdom.
[9] K. Greisen, Phys. Rev. Lett. **16** (1966) 748; G.T. Zatsepin and V.A. Kuzmin, Sov. Phys. JETP Lett. **4** (1966) 78.
[10] B. Dawson et al. for the Pierre Auger, Telescope Array and Yakutsk Collaborations, in International Symposium on Future Directions in UHECR physics (2012) CERN.
[11] P. Facal, for the Pierre Auger Collaboration, Proc. 32nd ICRC, Beijing, China (2011) and arXiv: 1107.4804.
[12] The Pierre Auger Collaboration, JCAP **1302** (2013) 026.
[13] D. Garcia-Pinto for the Pierre Auger Collaboration, Proc. 32nd ICRC, Beijing, China (2011) and arXiv: 1107.4804.
[14] D. Garcia-Gamez for the Pierre Auger Collaboration, Proc. 32nd ICRC, Beijing, China (2011) and arXiv: 1107.4804.
[15] A. M. Taylor, M. Ahlers, F. A. Aharonian, Phys. Rev D **84** (2011) 105007.
[16] D. Allard, Astrop. Phys. **39-40** (2012) 33.
[17] E. Barcikowski et al. for the Pierre Auger, Telescope Array and Yakutsk Collaborations, in International Symposium on Future Directions in UHECR physics (2012) CERN.
[18] G. Rodriguez for the Pierre Auger Collaboration, Proc. 32nd ICRC, Beijing, China (2011) and arXiv: 1107.4809.
[19] S. Ostapchenko, Phys. Lett. B **636** (2006) 40.
[20] A. Yushkov, for the Pierre Auger Collaboration, in International Symposium on Future Directions in UHECR physics (2012) CERN.
[21] K. Werner, F.-M. Liu, T. Pierog, Phys. Rev. C **74** (2006) 044902.
[22] P. Battacharije and G. Sigl, Phys. Rep. **327** (2000) 109.
[23] M. Galaverni and G. Sigl, Phys. Rev. Lett. **100** (2008) 021102.
[24] L. D. Landau, I.Ya. Pomeranchuk, Dokl. Acad. Nauk. **92** (1953) 553; A.B. Migdal, Phys. Rev. **103** (1956) 1811.
[25] D. Martello for the Pierre Auger Collaboration: 2009 in 7th Workshop on Gamma-ray Physics in the LHC Era, Assisi, Italy.
[26] The Pierre Auger Collaboration, Astrop. Phys. **31** (2009) 399; Astrop. Phys. **29** (2008) 243.
[27] V. Scherini for the Pierre Auger Collaboration, in International Symposium on Future Directions in UHECR physics (2012) CERN.
[28] The Pierre Auger Collaboration, Science **318** (2007) 938.
[29] M. P. Véron-Cetty, P. Véron, A&A 445 (2006) 773.
[30] K.-H. Kampert for the Pierre Auger Collaboration, Highlight talk in Proc. 32nd ICRC, Beijing, China (2011).
[31] O. Deligny et al. for the Pierre Auger, Telescope Array and Yakutsk Collaborations, in International Symposium on Future Directions in UHECR physics (2012) CERN.
[32] The Pierre Auger Collaboration, Astrop. Phys. **35** (2012) 354.
[33] The Pierre Auger Collaboration, ApJ **760** (2012) 148.
[34] The Pierre Auger Collaboration, Astrop. Phys. **34** (2011) 627.
[35] The Pierre Auger Collaboration, ApJ. Suppl. **203** (2012) 34; ApJ. Lett. **762** (2013) L13.